ELSEVIER

International Journal of Mass Spectrometry 217 (2002) 1–22

International Journal of Mass Spectrometry

www.elsevier.com/locate/ijms

Hydrogen-shift isomers of ionic and neutral hydroxypyridines: a combined experimental and computational investigation

Moschoula A. Trikoupis [a], Pascal Gerbaux [b,1], David J. Lavorato [a,2], Robert Flammang [b,3], Johan K. Terlouw [a,*]

[a] *Department of Chemistry, McMaster University, 1280 Main St. West, Hamilton, Ont., Canada L8S 4M1*
[b] *Organic Chemistry Laboratory, University of Mons-Hainaut, 19, Avenue Maistriau, Mons 7000, Belgium*

Received 4 July 2001; accepted 1 October 2001

In memory of Pierre Longevialle, a dear friend, who enjoyed gas-phase ion chemistry and made several seminal contributions to the field.

Abstract

Apart from pyridine N-oxide (**1a**), the C_5H_5NO family of stable molecules comprises, 2-, 3- and 4-hydroxypyridine (**2a**, **3a** and **4a**) as well as their keto counterparts 2-, 3- and 4(1*H*)-pyridone (**2b**, **3b** and **4b**). This study focuses on the characterisation of their radical cations and a number of stable H-shift isomers, which are α- or β-distonic ions. This was done by using a combination of mass spectrometric experiments and computational chemistry, at the B3LYP/CBSB7 level of theory. The ionic species were identified on the basis of both their collision-induced dissociation (CID) characteristics and specific associative ion–molecule reactions with dimethyl disulfide and *tert*-butyl isocyanide as substrates.

The distonic ions (**1b**$^{\bullet+}$, **2c**$^{\bullet+}$, **2d**$^{\bullet+}$ and **3c**$^{\bullet+}$) were obtained by dissociative electron impact ionisation and subjected to neutralisation–reionisation mass spectrometry (NRMS). From CID spectra of the intense survivor ions, it follows that the neutral counterparts of the α-distonic ions **2c**$^{\bullet+}$ and **3c**$^{\bullet+}$ are viable chemical species in the rarefied gas phase. The energy-rich ylide type neutrals **1b**, on the other hand, readily isomerise into pyridine N-oxide, **1a**, or else dissociate.

The neutral counterpart of the β-distonic ion **2d**$^{\bullet+}$ only has a marginal stability and part of these neutrals are proposed to isomerise into energy-rich 2-pyridone molecules **2b**. This is in agreement with the computational results. However, ionised 2-pyridone cannot readily be differentiated from its enol isomer 2-hydroxypyridine. In contrast, the keto isomers of ionised 3- and 4-hydroxypyridine display characteristically different CID spectra. (Int J Mass Spectrom 217 (2002) 1–22)

Keywords: Neutralisation–reionisation mass spectrometry; Associative ion–molecule reactions; Density-functional calculations; Hydroxypyridine; Distonic ions

1. Introduction

Proton transfer plays a key role in a wide range of chemical and biochemical processes. In particular, the proton transfer associated with keto–enol tautomerisations has long been of interest because such reactions may catalyse certain biochemical transformations [1]. In this context, the prototropic tautomerisation of

* Corresponding author. E-mail: terlouwj@mcmaster.ca
[1] Chargé de Recherches du Fonds National de la Recherche Scientifique.
[2] Present address: MDS Sciex, 71 Four Valley Drive, Concord, Ont., Canada L4K 4V8.
[3] E-mail: robert.flammang@umh.ac.be

1387-3806/02/$ – see front matter
PII S1387-3806(02)00531-6

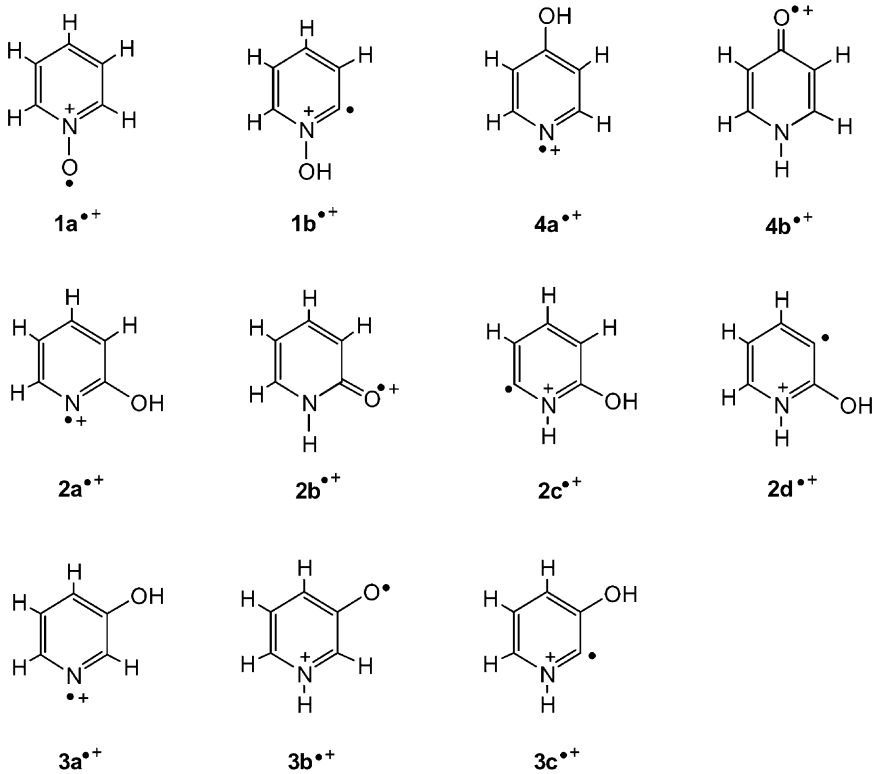

Scheme 1.

2- and 4-hydroxypyridine has been much studied [2]. A key feature of this system is that the gaseous enthalpies of formation of the two tautomeric forms, the pyridinol structures **2a**/**4a** vs. the pyridone structures **2b**/**4b** in Scheme 1, are closely similar. The 3-isomer on the other hand, exclusively exists as 3-hydroxypyridine, **3a**, because its keto counterpart, **3b**, is a betaine type molecule of much higher energy.

The chemical environment plays an important role in the tautomerism of 2- and 4-hydroxypyridine. For the 2-isomer, X-ray crystallography experiments revealed that 2-pyridone is the only tautomer present in the solid state [3]. It is also the preferred tautomer in aqueous solutions. This is readily understood in terms of solvation effects with the hydroxy form becoming the most important isomer in solvents of low polarity [4]. In the gas-phase, under conditions where an intermolecular proton transfer allows the tautomers to equilibrate, a variety of spectroscopic measurements (UV, IR and microwave spectroscopy), provide evidence that the hydroxy form dominates, representing roughly 75% of the population [5]. In the condensed phase, the 4-isomer also largely exists in the pyridone form. However, as shown by photoelectron spectroscopy, in the gaseous state at least 95% of the 4-isomer consists of the 4-hydroxypyridine tautomer [6].

This tautomerisation has also received considerable attention from computational chemistry [7]. The hydroxy forms of the 2- and 4-isomers are calculated to be slightly more stable than their keto structure, by 1–3 kcal/mol, respectively [7a,g]. For the 2-isomer, an experimental value of 1 kcal/mol has been reported [8]. Unlike the two 4-isomers, which can only equilibrate via an intermolecular proton transfer, the 2-isomers could interconvert via an intramolecular 1,3-H shift. However, computations at various levels

of theory all predict that the barrier associated with this shift is quite high, 38 kcal/mol at the CISD/DZP1 level of theory [7g].

The hydroxypyridines have also been extensively studied by mass spectrometry [9,10]. Early studies include analysis of deuterium isotope effects on the dissociation of the metastable molecular ions [10b] and ion–molecule reactions under conditions of chemical ionisation [10c]. These studies indicate that, prior to ionisation in the rarefied gas-phase, all three isomers exist in their pyridinol form and that the resulting hydroxypyridine radical cations are separated by a high 1,3-H shift barrier for the ketonisation. In a subsequent metastable ion study [11], it was concluded from an analysis of the metastable peak shape for loss of CO, that the ionised 2-isomer exists solely in its hydroxy form.

This result seems to be at odds with the spectroscopic evidence quoted above that, in the gas phase, the keto form comprises 25% of the sample population. One explanation is that under the experimental conditions used in mass spectrometry, the sample vaporises as the hydroxy form and does not equilibrate [6]. However, there is another possibility which will be discussed below.

Despite the interest in the tautomerisation of ionised hydroxypyridines, little or no information is available on the behaviour of their distonic H-shift isomers. Such ionic species (and some of their neutral counterparts) are well characterised by theory and experiment for simple heterocycles, including pyridine, pyrazine, pyrimidine and pyridazine [12].

In the present study, we focus on the dissociation chemistry and reactivity of the 2-, 3- and 4-hydroxypyridine ions and their keto counterparts vis-à-vis a number of other potentially stable H-shift isomers, viz. the α- and β-distonic ions shown in Scheme 1. An additional α-distonic isomer pertinent to this study is the 1,3-H shift isomer of pyridine N-oxide.

The experimental approach uses a variety of tandem mass spectrometry based techniques: metastable ion (MI) and collision-induced dissociation (CID) characteristics, neutralisation–reionisation mass spectrometry (NRMS) (for a recent review see [13]) and associative ion–molecule reactions [14]. In addition, collision-induced dissociation experiments (denoted as NR/CID experiments [12d]) were performed on those isomeric ions that survived the neutralisation–reionisation process. Such experiments not only provide information about the structure and stability of the neutral counterparts of the ion, they also probe the isomeric purity of the ions [12d]. To assist in the interpretation of the experimental observations, density functional theory calculations are used to obtain relative energies for the radical cations and neutrals and barriers for selected H-shifts.

2. Experimental

The tandem mass spectrometric experiments used to generate and characterise the C_5H_5NO ions and neutrals were performed at McMaster University on the VG Analytical ZAB-R. This BE_1E_2 (B: magnet, E: electric sector) instrument and the details of the NR mass spectrum acquisition have been previously described [15], hence only a brief overview is provided here. The ions of interest, e.g., *m/z* 95 in the case of $C_5H_5NO^{\bullet+}$, are mass-selected by B and subsequently (in a small gas cell located between B and E_1) subjected to collision with *N*,*N*-dimethylaniline. This results in neutralisation by fast electron transfer of a fraction of the 10 keV source generated ions. After exiting the cell, the remaining ions are deflected by a positively charged electrode so that only a beam of fast moving neutral species enters a second gas cell. Here reionisation takes place by collision with oxygen molecules. The resulting ions are analysed by scanning E_1 to produce the conventional NR mass spectrum. If instead the reionised species are selectively transmitted at a fixed E_1 setting, and oxygen gas is introduced in a third cell located between E_1 and E_2, a NR/CID mass spectrum characteristic of the reionised neutrals can be obtained by scanning E_1. Comparative CID experiments are performed analogously but with the deflector electrode switched off. Spectra were recorded with a PC-based data system (Mommers Technologies Inc., Ottawa, Canada).

Samples were introduced into the mass spectrometer via an all-glass heated inlet system equipped with a leak valve or a direct insertion-type probe. At indicated pressures (monitored by a remote ionisation gauge) of typically 10^{-6} Torr, ions were formed by electron ionisation (70 eV) at a source temperature of 120 °C.

The ion–molecule reaction spectra were recorded on a six sector tandem mass spectrometer (Micromass Autospec 6F, Manchester) of $c_1E_1B_1c_2E_2c_3c_4E_3B_2c_5E_4$ geometry (E: electric sector, B: magnetic sector, c: collision cell) [16] at the University of Mons. General conditions were 8 kV accelerating voltage, 200 μA trap current (in the electron ionisation mode, EI), 1 mA (in the chemical ionisation mode, CI), 70 eV ionising electron energy and 200 °C ion source temperature. The solid samples were introduced with a direct insertion probe, while the liquid samples were injected into the ion source via a heated (180 °C) septum inlet.

The instrument has been modified with an rf-only quadrupole collision cell (Q cell) between E_2 and E_3 as has been reported elsewhere [16b]. This modification allows the study of associative ion–molecule reactions and the study of collision-induced dissociation of decelerated ions having 20–30 eV kinetic energy. Briefly, the experiments utilising the quadrupole consist of the selection of a beam of fast moving ions (8 keV) with the three first sectors ($E_1B_1E_2$), the deceleration of these ions to approximately 5 eV (to maximise ion–molecule reactions) or 20–30 eV (to maximise collision-induced dissociations). The interaction between the ions and the reagent gas (the pressure of the gas is estimated to be ca. 10^{-3} Torr) is thereafter realised in the Q cell and, after reacceleration to 8 keV, all the ions generated in the quadrupole are separated and mass measured by scanning the field of the second magnet. The high-energy CID spectra of mass-selected ions generated in the Q cell can be recorded by a linked scanning of the fields of the three last sectors. The pressure of the neutral reagent in the quadrupole collision cell cannot be reliably measured as it is estimated using an ionisation gauge situated quite far away from the quadrupole cell. For the sake of consistency, an ion transmission of 50% was used in all experiments.

All compounds were purchased from commercial sources and used without further purification.

3. Results and discussion

3.1. Computation of energies for the $C_5H_5NO^{\bullet+}$ isomers and their neutral counterparts

The potential energy surface comprising the $C_5H_5NO^{\bullet+}$ radical cations **1**$^{\bullet+}$–**4**$^{\bullet+}$ of Scheme 1, as well as that of the corresponding neutrals and selected connecting transition structures of the 1,3-H shifts, was explored at a level of theory (B3LYP/CBSB7) that has proven adequate for related species [12e]. This level of theory is also used in the CBS-QB3 model chemistry [17]. The calculations were performed on a PC using the Gaussian 98W program [18]. Analytical frequency calculations confirmed the assignment of stable or transition structures based on the correct number of negative eigenvalues of the Hessian matrix, 0 or 1, respectively. The geometric parameters (which are not presented but are available upon request) and energies of the structures were obtained with the CBSB7 basis set using the standard hybrid density functional theory option (HF/DFT) designated B3LYP [19]. Relative energies were corrected for non-scaled zero-point vibrational energy (ZPVE) contributions. All $\langle s^2 \rangle$ expectation values of the open shell systems were within 5% of the expected value and show that the B3LYP wave functions do not suffer appreciably from spin contamination.

The energy data for the isomeric ions and their neutral counterparts are collected in Table 1. Among the H-shift isomers of ionised 2-hydroxypyridine, **2a**$^{\bullet+}$, the keto isomer **2b**$^{\bullet+}$ is the most stable species. It is calculated to lie 11.5 kcal/mol lower in energy than the pyridinol ion **2a**$^{\bullet+}$, in satisfactory agreement with a recent ZEKE photoelectron spectroscopic measurement which found the difference in the two ionic species to be 0.5 eV in favour of **2b**$^{\bullet+}$ [20]. The transition state for the 1,3-H shift connecting **2a**$^{\bullet+}$ and **2b**$^{\bullet+}$

Table 1
Calculated energies (B3LYP/CBSB7) for the selected isomerisation barriers for 1,3-hydrogen migrations

Species	Hartree[a]	ZPVE (kcal/mol)	E_{rel} (kcal/mol)[b]
$C_5H_5NO^{\bullet+}$ ions $\mathbf{1}^{\bullet+}$–$\mathbf{4}^{\bullet+}$			
$\mathbf{2a}^{\bullet+}$	−323.286262	57.5	0.0
$\mathbf{2b}^{\bullet+}$	−323.304605	57.8	−11.2
$\mathbf{2c}^{\bullet+}$	−323.263124	57.6	14.6
$\mathbf{2d}^{\bullet+}$	−323.271971	58.2	9.7
$\mathbf{3a}^{\bullet+}$	−323.270412	56.9	9.3
$\mathbf{3b}^{\bullet+}$	−323.289970	57.7	−2.1
$\mathbf{3c}^{\bullet+}$	−323.259365	58.0	17.4
$\mathbf{4a}^{\bullet+}$	−323.265260	56.6	12.3
$\mathbf{4b}^{\bullet+}$	−323.285058	58.3	1.6
$\mathbf{1a}^{\bullet+}$	−323.232927	57.5	33.5
$\mathbf{1b}^{\bullet+}$	−323.193687	56.8	57.4
TS $\mathbf{2a}^{\bullet+} \rightarrow \mathbf{2b}^{\bullet+}$	−323.237256	54.4	27.7
TS $\mathbf{1a}^{\bullet+} \rightarrow \mathbf{1b}^{\bullet+}$	−323.125811	53.3	96.3
C_5H_5NO neutrals **1–4**			
2a	−323.605640	58.0	0.0
2b	−323.607008	58.0	−0.9
2c	−323.524243	57.5	50.6
2d	−323.520109	57.6	53.3
3a	−323.589567	57.5	9.6
3b	−323.569299	57.8	22.6
3c	−323.533444	58.0	45.3
4a	−323.593277	57.7	7.5
4b	−323.590992	57.9	9.1
1a	−323.531436	57.5	46.1
1b	−323.477795	56.9	79.1
TS **2a** → **2b**	−323.547497	54.8	33.3
TS **1a** → **1b**	−323.449632	54.2	94.1
TS **2b** → **2d**	−323.495113	54.8	66.2

[a] Doublet (Hartree) for $C_5H_5NO^{\bullet+}$ ions $\mathbf{1}^{\bullet+}$–$\mathbf{4}^{\bullet+}$ and singlet (Hartree) for C_5H_5NO neutrals **1–4**.
[b] Relative energies are corrected for zero-point vibrational energy (ZPVE).

was also calculated. The barrier for the interconversion is substantial, 28 kcal/mol relative to $\mathbf{2a}^{\bullet+}$, so that the keto ion may well be an observable species in the gas-phase.[4] This point will be further addressed in Section 3.3. The distonic ions, $\mathbf{2c}^{\bullet+}$ and $\mathbf{2d}^{\bullet+}$, are both stable species but they lie higher in energy, by ca. 10–15 kcal/mol, than the 2-hydroxypyridine ion. This contrasts with the pyridine system where ionised pyridine and its distonic H-shift isomers are comparable in stability. For the neutral counterparts of $\mathbf{2}^{\bullet+}$, our calculations predict the keto and enol forms to be of comparable stability, in agreement with experiment. The α-ylide **2c** and the zwitterion **2d** are both calculated to be stable species but, not surprisingly, they lie considerably higher in energy, by ca. 50 kcal/mol. Consequently, their IEs, see Table 2, are considerably lower than those of their conventional isomers **2a**/**b**. This difference in IE provides an important criterion for isomer differentiation by ion–molecule reactions as discussed in Section 3.4.

For the 3-isomers, neutral 3-hydroxypyridine, **3a**, is predicted to be considerably more stable than its highly polar pyridone tautomer **3b**, by 13 kcal/mol.

[4] The height of the barrier was also calculated using the CBS-QB3 method [17]. The UMP2 and UMP4 single point calculations within this collective method suffered from large spin contamination and in place of their energies, the projected energies (PMP2 and PMP4), where the higher spin component is projected out, were used. The relative energy obtained using this strategy agreed within 2 kcal/mol with that from the B3LYP/CBSB7 procedure.

Table 2
Calculated (B3LYP/CBSB7) recombination (RE) and ionisation (IE) energies (eV) of the C_5H_5NO isomers of Scheme 1

Species	RE (vertical)	IE (adiabatic)	IE (vertical)
1a	8.1	8.1 (8.4)[a]	8.2
1b	7.2	7.7	8.2
2a	8.5	8.7 (8.9)	8.9 (9.1)[b]
2b	8.1	8.2 (8.4)	8.4 (8.6)
2c	6.4	7.1	7.5
2d	6.3	6.8	7.2
3a	8.4	8.7 (9.1)	8.9 (9.1)
3b	7.5	7.6	7.7
3c	7.0	7.5	8.0
4a	8.4	8.9 (9.7)	9.5 (9.8)
4b	8.1	8.3	8.5

[a]Experimental values quoted in [21], with the exception of IE **2a**/**2b** which were taken from the ZEKE PES study of [20].
[b]Experimental values form the PES study of [6].

Upon ionisation there is a reversal of stabilities and the betaine-type ion $\mathbf{3b}^{\bullet+}$ is calculated to lie as much as 10 kcal/mol lower in energy than $\mathbf{3a}^{\bullet+}$. The distonic H-shift isomer, $\mathbf{3c}^{\bullet+}$, is of comparable stability, but its neutral counterpart, the α-ylide **3c**, lies 35 kcal/mol higher in energy than **3a**.

The 4-isomers behave analogously to the 2-isomers: their neutral forms are comparable in stability while the energy between the two ions is larger, 11 kcal/mol in favour of the keto ion $\mathbf{4b}^{\bullet+}$.

The doublet states of $\mathbf{1a}^{\bullet+}$ and $\mathbf{1b}^{\bullet+}$ differ by 24 kcal/mol, and thus, the pyridine N-oxide ion is considerably more stable than its α-ylide isomer. However, a facile isomerisation via a 1,3-H shift is prohibited by a high barrier, TS ($\mathbf{1b}^{\bullet+} \rightarrow \mathbf{1a}^{\bullet+}$) is 39 kcal/mol, and thus, the ylide ion $\mathbf{1b}^{\bullet+}$ should be a viable species in the gas-phase. Upon neutralisation, the energy difference between the two isomers remains approximately the same, 33 kcal/mol, but the connecting TS (**1b** → **1a**) is much lower, 15 kcal/mol. Such a relatively low barrier may not be sufficient to prevent a (partial) isomerisation into the more stable isomer when ions $\mathbf{1b}^{\bullet+}$ are neutralised in a NRMS experiment. The neutralisation step in such an experiment is a vertical process [13]. Therefore, energy-rich neutrals are generated if the geometries of the ion and its corresponding ground state neutral differ considerably.

To gauge the importance of this effect, we have obtained the Franck–Condon recombination energies, RE_v, for the neutralisation of the ions by vertical electron capture. This was done by calculating the difference in energy between the ion and the neutral using the optimised geometry of the ion. The RE_v value derived from this calculation is then compared with the adiabatic ionisation/recombination energy. The results are tabulated in Table 2. From the difference between IE_a and RE_v, 11 kcal/mol (0.5 eV), it follows that the vertical neutralisation of ions $\mathbf{1b}^{\bullet+}$ is expected to yield energy-rich neutrals **1b**. Considering that the isomerisation barrier **1b** → **1a** is fairly low, see above, neutralised ions $\mathbf{1b}^{\bullet+}$ may well undergo a partial isomerisation.

The same may hold for the distonic ion $\mathbf{2d}^{\bullet+}$: from the results in Table 2 it follows that its neutral counterpart is generated with at least 0.5 eV excess energy while the barrier for isomerisation into its keto isomer **2b** is fairly low, TS (**2d** → **2b**) is 13 kcal/mol.

3.2. Generation of the $C_5H_5NO^{\bullet+}$ radical cations

The pyridine N-oxide radical cation $\mathbf{1a}^{\bullet+}$, and the three isomeric hydroxypyridine ions $\mathbf{2a}^{\bullet+}$, $\mathbf{3a}^{\bullet+}$ and $\mathbf{4a}^{\bullet+}$ were generated by electron impact (EI) ionisation of their neutral counterparts. Considering, see Section 1, that for 2-hydroxypyridine a substantial amount of the keto isomer may co-exist in the vapour phase, ions of putative structure $\mathbf{2a}^{\bullet+}$ were also generated by the dissociative ionisation of *N*-propyl 2-pyridone, **I**, as shown in Scheme 2. Since the keto ion $\mathbf{2b}^{\bullet+}$ is predicted by theory to be considerably more stable than its enol counterpart, $\mathbf{2a}^{\bullet+}$, we have also entertained the possibility that this ion may be generated by loss of C_2H_4 from ionised 2-ethoxypyridine, $\mathbf{II}^{\bullet+}$. However, see Scheme 2, this precursor molecule could also yield ions $\mathbf{2a}^{\bullet+}$ (via a β-H transfer to the ether oxygen atom) or a mixture of $\mathbf{2a}^{\bullet+}$ and $\mathbf{2b}^{\bullet+}$. The keto counterparts of $\mathbf{3a}^{\bullet+}$ and $\mathbf{4a}^{\bullet+}$ are also predicted by theory to be lower in energy than their enol counterparts but suitable precursor molecules for their generation by dissociative ionisation could not be envisaged. Guided by

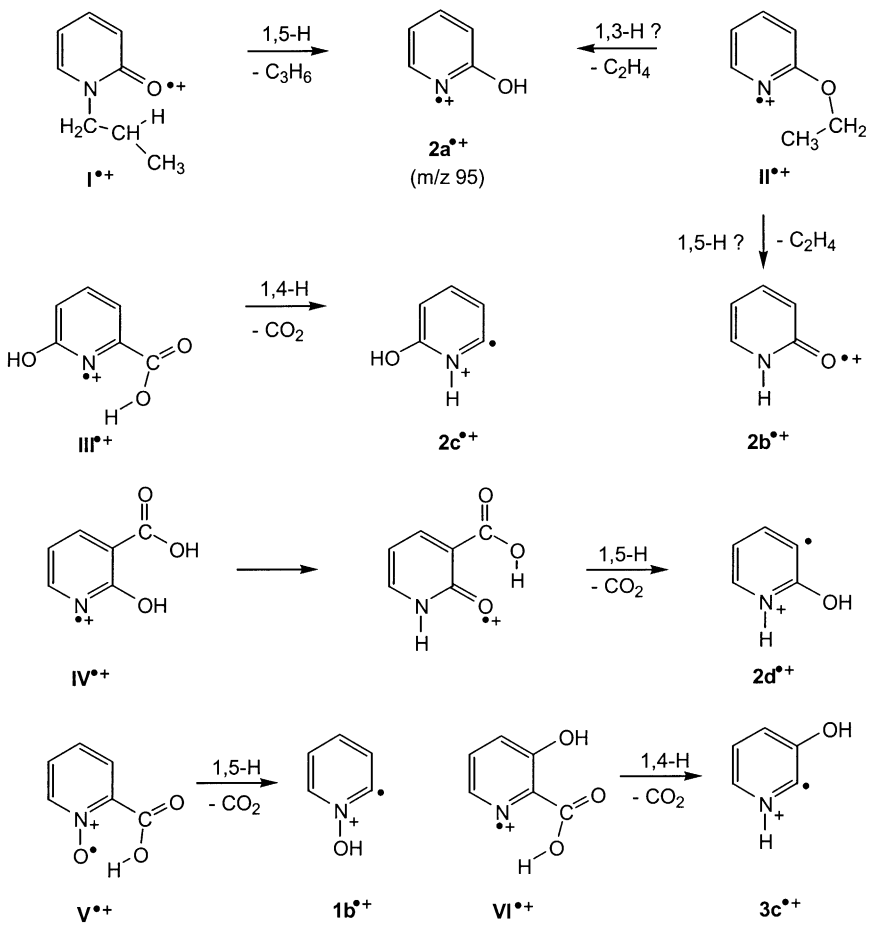

Scheme 2.

earlier work on the generation of various distonic ions derived from simple N-heterocycles [12], we envisaged that the distonic ions **1b**$^{\bullet+}$, **2c**$^{\bullet+}$, **2d**$^{\bullet+}$ and **3c**$^{\bullet+}$ should be obtainable by dissociative electron ionisation via the pathways shown in Scheme 2.

3.3. Characterisation of the C_5H_5NO radical cations and neutrals on the basis of their dissociation reactions

The CID mass spectra of the various isomeric ions are presented in the left hand columns of Fig. 1(a and b). Fig. 2 presents the corresponding NRMS, whereas the right hand columns of Fig. 1(a and b) display the CID spectra of the survivor ions in these NR spectra. In a recent CID study [22], it was shown that oxygen as a collision gas greatly enhances the structure diagnostic loss of O (peak at *m/z* 79) from the pyridine N-oxide radical cations **1a**$^{\bullet+}$. We have therefore, obtained all three sets of spectra with O_2 as the target gas.

3.3.1. The dissociation characteristics of the radical cations of pyridine N-oxide and the three hydroxypyridine isomers

It is readily seen from Fig. 1(a and b), that the CID spectra of the isomers of conventional structure, viz. those of **1a**$^{\bullet+}$, **2a**$^{\bullet+}$, **3a**$^{\bullet+}$ and **4a**$^{\bullet+}$, are distinctly different. The same holds for their NR spectra which,

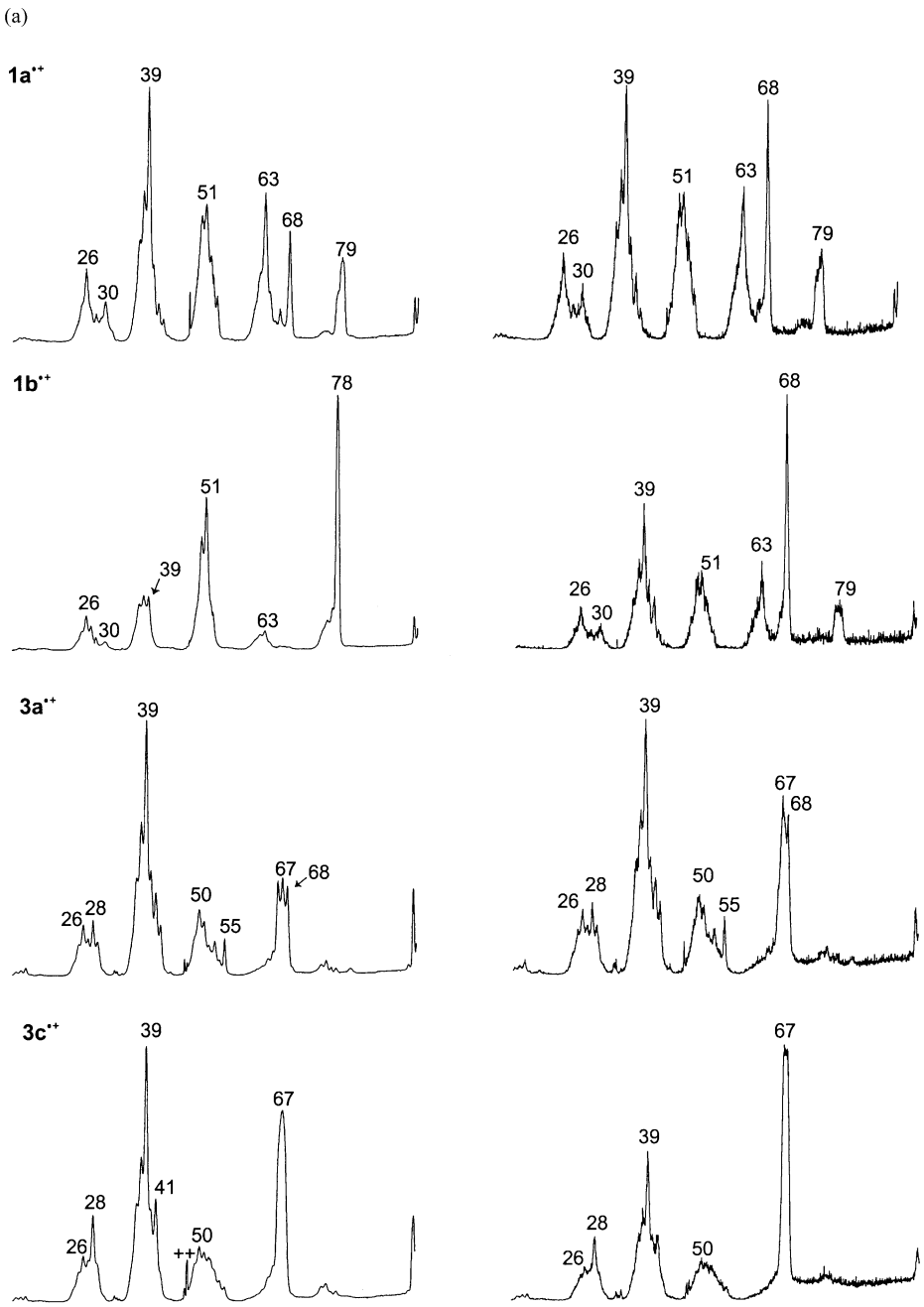

Fig. 1. (a) 10 keV CID mass spectra of source generated ions (3ffr, left hand column) and survivor ions generated in the neutralisation–reionisation experiments depicted in Fig. 2 (right hand column). (b) 10 keV CID mass spectra of source generated ions (3ffr, left hand column) and survivor ions generated in the neutralisation–reionisation experiments depicted in Fig. 2.

(b)

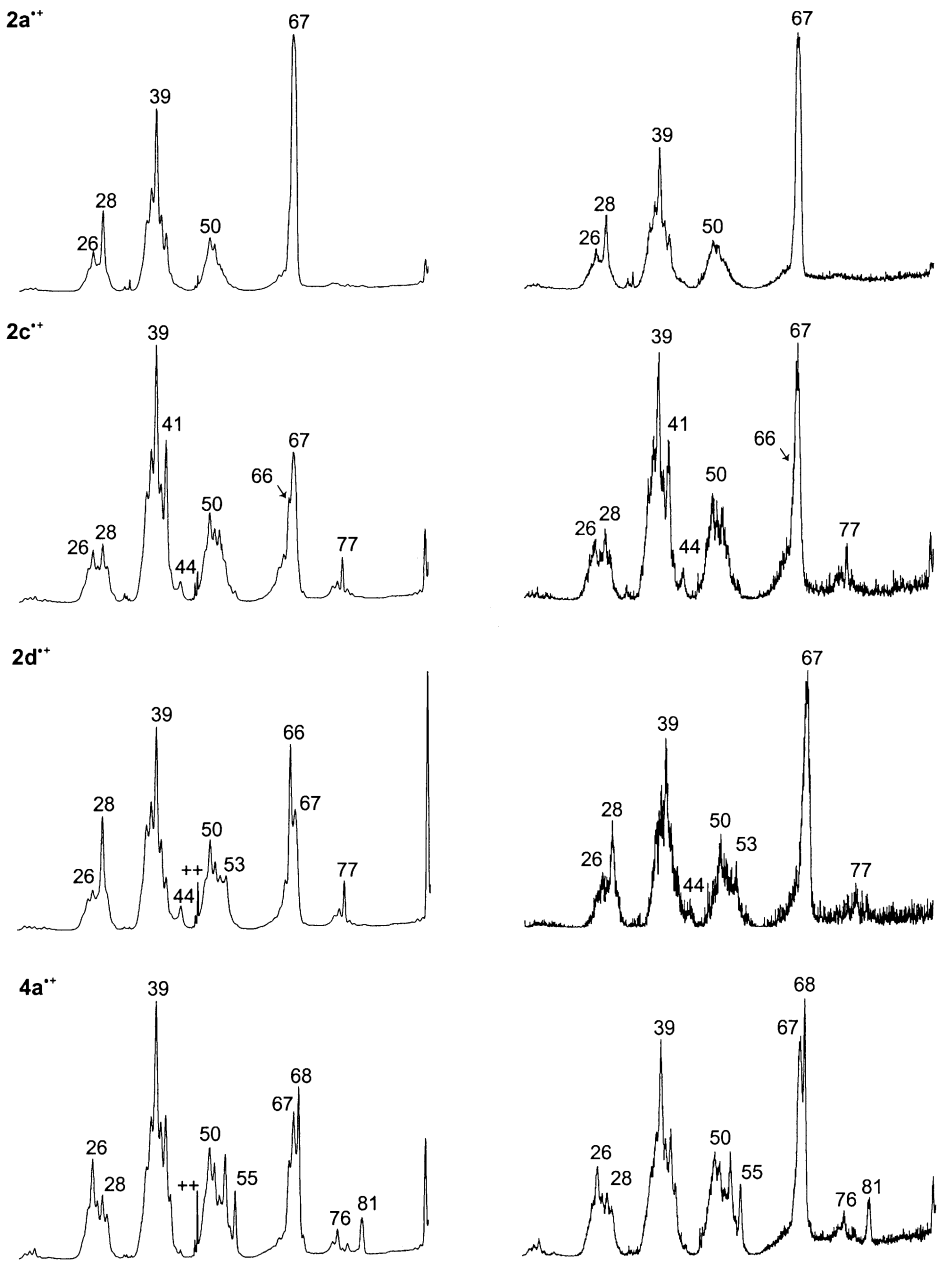

Fig. 1. (*Continued*).

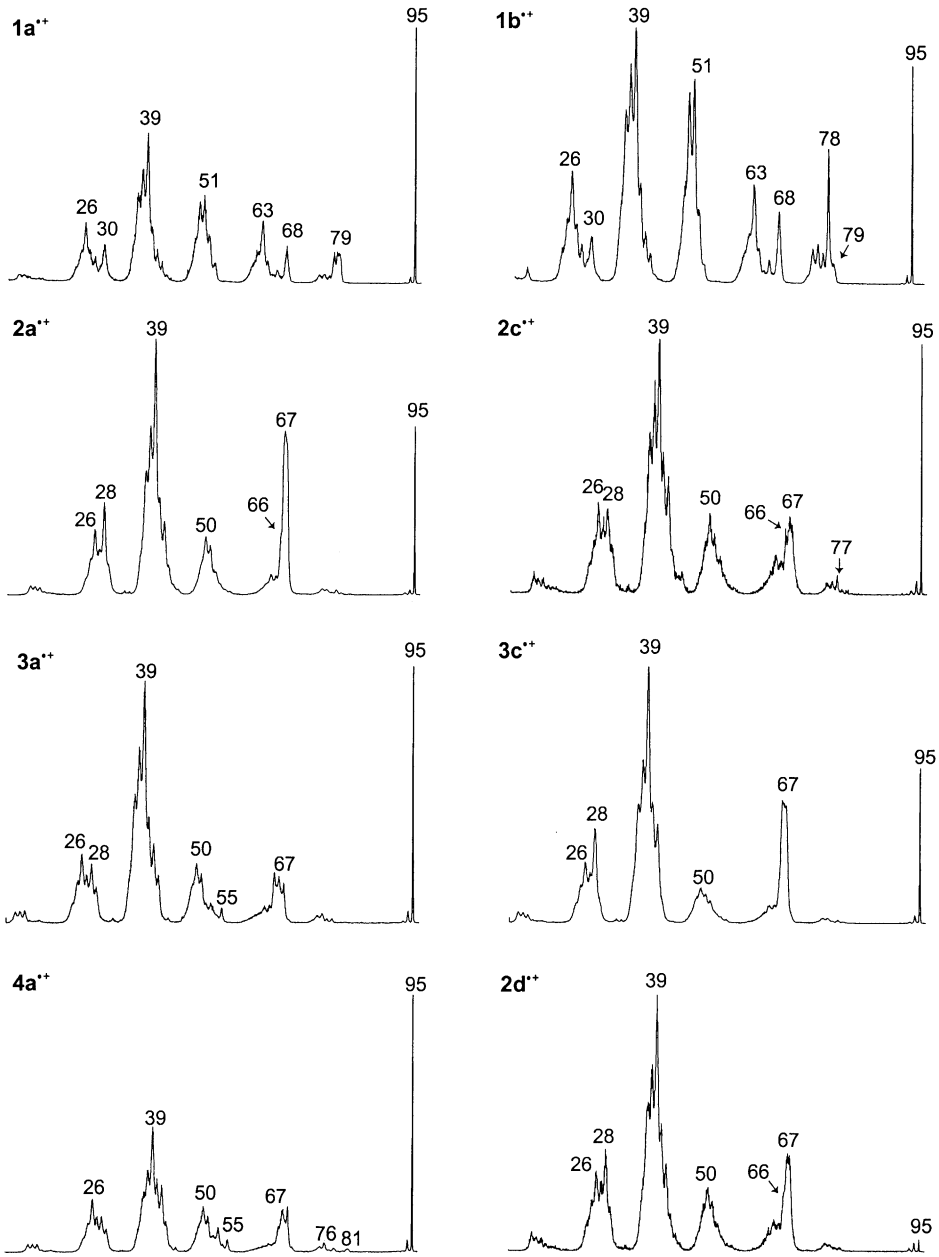

Fig. 2. 10 keV neutralisation–reionisation mass spectra of source generated ions (2ffr).

see Fig. 2, display prominent "recovery" or "survivor ion" signals at *m/z* 95. The CID spectra of these survivor ions, the NR/CID spectra of Fig. 1(a and b), right column, are closely similar to the CID spectra of the source generated ions. The only notable difference(s) lie in the enhanced intensity of the *m/z* 68 peak in the NR/CID spectrum of $\mathbf{1a}^{\bullet+}$, *m/z* 67 in that of $\mathbf{2a}^{\bullet+}$ and *m/z* 67/68 in those of $\mathbf{3a}^{\bullet+}$ and $\mathbf{4a}^{\bullet+}$. However,

this merely reflects the somewhat higher internal energy content of ions generated by the NR sequence: such ions contain a larger fraction of metastable ions that dissociate via the reaction(s) of lowest energy requirement [12]. Indeed, metastable ions $\mathbf{1a}^{\bullet+}$ predominantly lose HCN to yield *m/z* 68 $C_4H_4O^{\bullet+}$ ions, whereas the low energy ions $\mathbf{2a}^{\bullet+}$, $\mathbf{3a}^{\bullet+}$ and $\mathbf{4a}^{\bullet+}$ readily decarbonylate to yield *m/z* 67 $C_4H_5N^{\bullet+}$ product ions. Metastable ions $\mathbf{3a}^{\bullet+}$ and $\mathbf{4a}^{\bullet+}$, but not $\mathbf{2a}^{\bullet+}$, also undergo a competing loss of HCN to yield *m/z* 68 ions. This close similarity between the CID and NR/CID spectra for the intensity distributions of the product ions resulting from the high energy dissociation reactions, attests to the isomeric purity of the source generated ions. In other words, stable ions $\mathbf{1a}^{\bullet+}$, $\mathbf{2a}^{\bullet+}$, $\mathbf{3a}^{\bullet+}$ and $\mathbf{4a}^{\bullet+}$ retain their structure integrity, and any isomerisation that is observed in the CID spectrum results from post-collisional isomerisation.

This conclusion is undoubtedly warranted for ions $\mathbf{1a}^{\bullet+}$ and also the hydroxypyridine isomers $\mathbf{3a}^{\bullet+}$ and $\mathbf{4a}^{\bullet+}$. The latter two isomers, either as metastable ions or else as stable ions energised by collisional activation, competitively lose HCN and CO. The decarbonylation reaction obviously requires a 1,3-H shift and is associated with a large kinetic energy release. The intermediate ions resulting from the 1,3-H shift are clearly high-energy species which upon ring-opening decarbonylate to yield 3-H pyrrole ions (from $\mathbf{4a}^{\bullet+}$) or a mixture of 2- and 3-H pyrrole ions (from $\mathbf{3a}^{\bullet+}$), as evidenced by a CID study of the product ions [10e].

However, an entirely different situation obtains for the 2-hydroxypyridine isomer $\mathbf{2a}^{\bullet+}$. Here, decarbonylation is the only low energy reaction observed in the MI spectrum and unlike the situation with ions $\mathbf{3a}^{\bullet+}$ and $\mathbf{4a}^{\bullet+}$, the 1,3-H transfer that initiates the decarbonylation does not yield a high energy intermediate ion but rather the more stable keto ion $\mathbf{2b}^{\bullet+}$! Scheme 3 summarises the information available on the decarbonylation of $\mathbf{2a}^{\bullet+}$: theory indicates that the reaction is associated with a ketonisation barrier of 28 kcal/mol and the CID study of [10e] leaves little doubt that the product ions have the 1-H pyrrole structure. The reaction is associated with a dished metastable peak

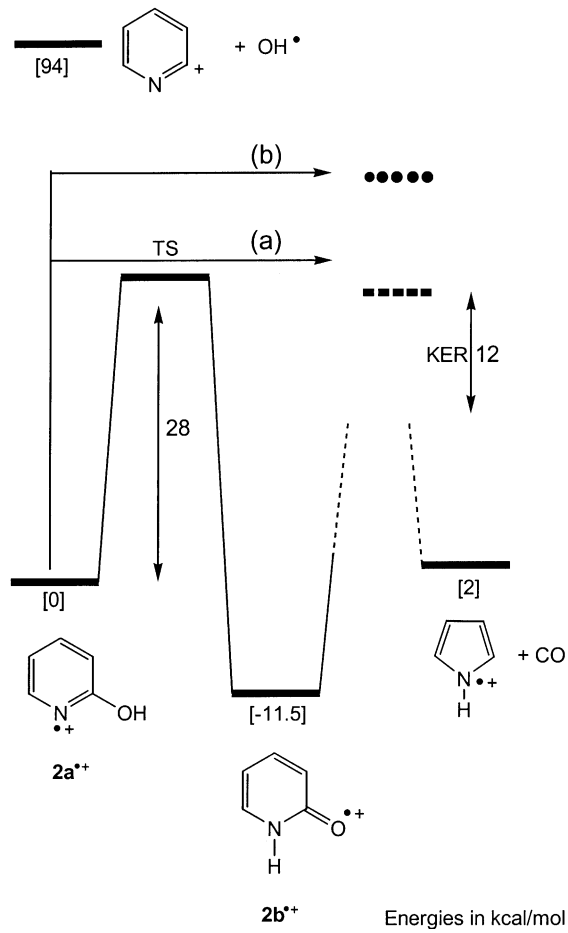

Scheme 3.

[23] whose half height kinetic energy release, $T_{0.5}$, is 520 meV (12 kcal/mol). Baldwin and Langley [11] have argued that this large energy release and the fact that the metastable peak shape is non-composite, provides strong evidence that the stable ions generated by EI of 2-hydroxypyridine all have the structure $\mathbf{2a}^{\bullet+}$ and that ketonisation only takes place en route to their dissociation, i.e., via pathway (a) in Scheme 3. Note that in this scenario the final step in the decarbonylation, $\mathbf{2b}^{\bullet+} \rightarrow$ 1-H pyrrole$^{\bullet+}$ + CO, can have a significant reverse activation energy. However, it should not exceed the level indicated by the bold squares (■) in Scheme 3.

To further probe this point, we have compared the MI, CID and NR/CID spectra of ionised 2-hydroxypyridine with those of the **2a**$^{\bullet+}$/**2b**$^{\bullet+}$ type ions generated via the dissociative ionisation routes depicted in Scheme 2. It appears that the resulting spectra are virtually identical.

One interpretation of these results is that we are dealing with stable ions **2a**$^{\bullet+}$ only. This implies that (i) direct ionisation of 2-hydroxypyridine yields enol ions **2a**$^{\bullet+}$ only and thus the neutral molecules generated by evaporation of the solid 2-pyridone sample in the rarefied gas-phase of the ion source are 2-hydroxypyridine molecules that cannot equilibrate with their keto form; (ii) the 2-ethoxypyridine ions do not yield the more stable keto ion via a 1,5-H shift but rather the enol ion via a β-hydrogen transfer. This is surprising since a 1,5-H shift generally is less energy demanding than a 1,3-H transfer. On the other hand, it follows from the PES study of [6] that the state that would best accommodate the 1,5-H transfer to N, the n_N state, lies ca. 1 eV above the ground state of the ion.

Another scenario, depicted as pathway (b) in Scheme 3, is that decarbonylation of the keto ions **2b**$^{\bullet+}$ into 1-H pyrrole product ions is associated with a barrier for the reverse reaction that lies considerably above the ketonisation barrier **2a**$^{\bullet+}$ → **2b**$^{\bullet+}$.

Considering that two bonds need to be broken and one is being formed to close the pyrrole ring, it is not without precedent that there be a high barrier associated with this dissociation. One such case is the loss of N_2 from the pyridazine radical cation which occurs via a barrier of ca. 2 eV [24]. Another example concerns the decarbonylation of 2- and 4-pyrone radical cations into ionised furan. Here too, the dissociations involve substantial reverse activation energies, 25–40 kcal/mol, respectively, as further exemplified by the broad metastable peaks [25].

In this scenario, enol and keto ions would show the same metastable characteristics. A mixture of the two ions could perhaps also remain undetected by the CID experiments reported above. Comparison of the CID and NR/CID spectra of a given ion can be advantageously used to probe its isomeric purity but only if its recombination and ionisation energies are largely different from those of the potential isomeric impurities. When dealing with ions of a conventional structure in admixture with their distonic counterparts (or vice versa) this criterion is readily fulfilled. For the present system, the RE and IE values of the two isomers, see Table 2, are not greatly different. Moreover, isomer differentiation by this procedure is greatly facilitated if the isomers have at least one structure diagnostic peak in their respective CID spectra. This unfortunately does not pertain to this system either: loss of $^{\bullet}$OH from **2a**$^{\bullet+}$ to yield *m/z* 78 α-pyridyl cations[5] lies far too high in energy, see Scheme 3, to compete with other non-structure diagnostic dissociations, as witnessed by its very low abundance in the spectra of all three hydroxypyridine isomers.

Demethylation upon collisional activation of protonated 2-methoxypyridine, as depicted in the upper part of Scheme 4, could provide an independent route to the generation of keto ions **2b**$^{\bullet+}$.

Under chemical ionisation conditions, using acetone or pyridine as the reagent gas, 2-methoxypyridine is readily protonated at the N-moiety and the resulting mass selected 10 keV *m/z* 110 ions were collisionally decomposed in the 2ffr. Similar experiments were performed with the 3- and 4-methoxypyridines. When collisionally energised, all three protonated molecules readily undergo demethylation to yield *m/z* 95 ions (see Fig. 3). These *m/z* 95 putative keto ions were then transmitted to the 3ffr to obtain their CID mass spectra which are presented in the right hand column of Fig. 3. From a comparison with the CID spectra of the hydroxy isomers **2a**$^{\bullet+}$, **3a**$^{\bullet+}$ and **4a**$^{\bullet+}$ in Fig. 1, it follows that the keto isomers **3b**$^{\bullet+}$ and **4b**$^{\bullet+}$ generated by the CI-CID sequence indeed have a unique CID spectrum. This is exemplified by a low *m/z* 26: *m/z* 28 ratio, in keeping with the fact that the keto ions **3b**$^{\bullet+}$ and **4b**$^{\bullet+}$ can readily generate HC≡NH$^+$.

In contrast, the CID spectrum of the keto ion **2b**$^{\bullet+}$ is indistinguishable from that shown in Fig. 1 for the enol ion **2a**$^{\bullet+}$. It could be argued, see Scheme 4,

[5] The 298 K enthalpy for this ion, 267 kcal/mol, was obtained from a CBS-QB3 calculation [17].

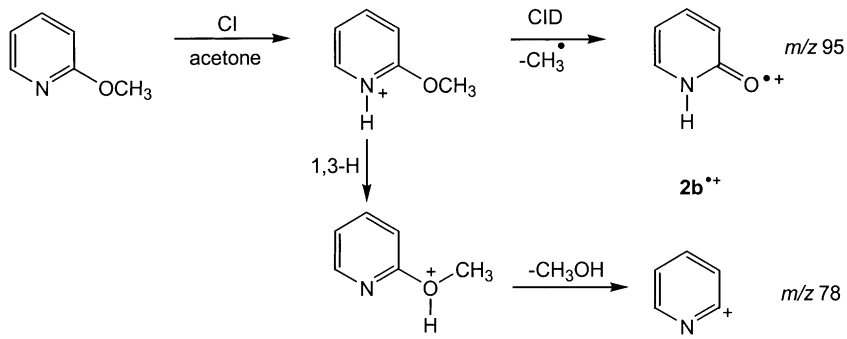

Scheme 4.

that the demethylation in this case takes place from the intermediate O-protonated ion which serves as the precursor for the loss of CH_3OH, yielding the intense signal at *m/z* 78 in Fig. 3(a). However, when pyridine-d_5 is used to form the N-D isotopologue, loss of CH_3OD suffers from a pronounced isotope effect whereas the demethylation does not. Thus, it is likely that keto ions **2b**$^{\bullet+}$ are indeed generated in the CI-CID sequence and considering that their spectrum is indistinguishable from that of the enol type ions, scenario (b) in Scheme 3 emerges as the most likely option.

Nevertheless, we feel that this intriguing problem can only be settled when an accurate appearance energy measurement and/or an elaborate computational study at a high level of theory becomes available.

3.3.2. The dissociation characteristics of the distonic ions and the stability of their neutral counterparts

The MI spectrum of the α-ylide ions **1b**$^{\bullet+}$ displays a single peak at *m/z* 78, corresponding to the loss of OH$^{\bullet}$. This observation clearly differentiates these ions from their isomer of conventional structure, **1a**$^{\bullet+}$. It further follows that ions **1b**$^{\bullet+}$ do not readily communicate with 2-hydroxypyridine ions **2a**$^{\bullet+}$, via a simple 1,2-OH shift. As discussed above, loss of OH$^{\bullet}$ from **2a**$^{\bullet+}$ has a minimum energy requirement of ∼94 kcal/mol, which greatly exceeds that associated with its decarbonylation (see Scheme 3). Consequently, metastable ions **2a**$^{\bullet+}$ exclusively lose CO and even upon collisional activation the loss of OH$^{\bullet}$ is of only marginal importance. Ions **1b**$^{\bullet+}$, however, lie much higher in energy than **2a**$^{\bullet+}$, by 57 kcal/mol, and are therefore, closer to the threshold for the generation of the α-pyridyl cation at *m/z* 78.

The two isomers, **1a**$^{\bullet+}$ and **1b**$^{\bullet+}$, also show significant differences in their CID spectra. The signals at *m/z* 30 (NO$^{\bullet+}$), 68 (–HCN) and 79 (–O$^{\bullet}$) are tell-tale peaks in the CID spectrum of **1a**$^{\bullet+}$, whereas loss of $^{\bullet}$OH dominates the CID spectrum of **1b**$^{\bullet+}$. These observations leave little doubt that the ylide ions **1b**$^{\bullet+}$ are stable species in the gas-phase, which do not tautomerise via a 1,3-H shift into pyridine N-oxide ions **1a**$^{\bullet+}$. For the behaviour of the neutral ylide, the NR and NR/CID spectra tell a different story. The CID and NR/CID spectra of ions **1a**$^{\bullet+}$ are virtually the same but this is clearly not the case for ions **1b**$^{\bullet+}$: the CID spectrum of the intense survivor ions in the NR spectrum of **1b**$^{\bullet+}$ is not that of ions **1b**$^{\bullet+}$, but rather that of ions **1a**$^{\bullet+}$. Thus, ions **1b**$^{\bullet+}$ which survived the neutralisation step of the NR experiment have isomerised into their more stable neutral tautomer **1a** prior to collisional ionisation. The presence of signature peaks for **1a**$^{\bullet+}$, *m/z* 79 and *m/z* 68, in the NR spectrum of **1b**$^{\bullet+}$ supports this proposal. Nevertheless, the NR spectrum of **1b**$^{\bullet+}$ also contains a sizeable peak at *m/z* 78, the signature peak of ions **1b**$^{\bullet+}$, which seems to suggest that part of the incipient neutrals **1b** retain their structure integrity on the μs time-frame of the NR experiment. A closer examination of the shapes of the *m/z* 78 peaks in the CID and NR spectra of **1b**$^{\bullet+}$ shows that this is not the case. The *m/z* 78 peak in the CID

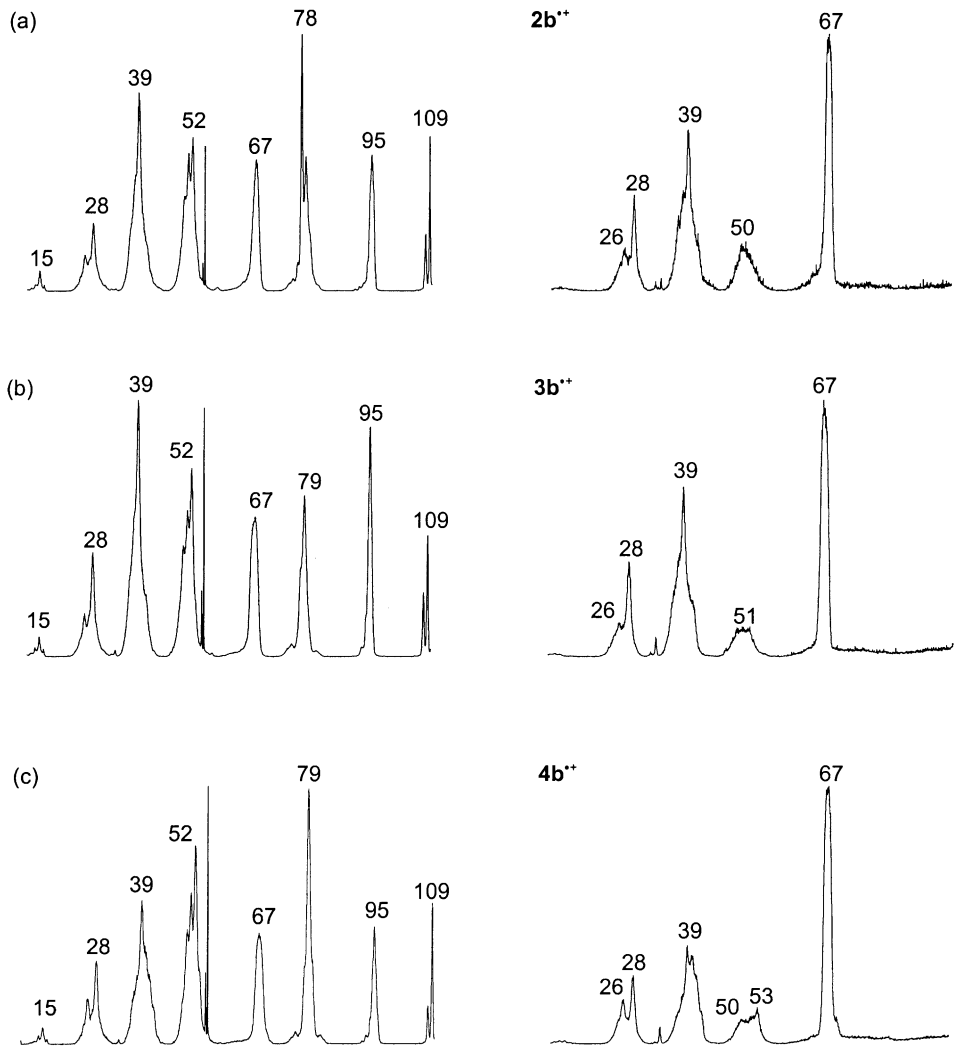

Fig. 3. 10 keV CID mass spectra of the *m/z* 110 protonated 2-, 3-, and 4-methoxypyridines, items (a), (b) and (c), and the *m/z* 95 of putative structures $\mathbf{2b}^{\bullet+}$, $\mathbf{3b}^{\bullet+}$ and $\mathbf{4b}^{\bullet+}$ ions generated therefrom.

spectrum is considerably broader than that displayed in the NR spectrum: the width at half height of the two peaks differs by almost a factor of 2. Thus, the *m/z* 78 peak in the NR spectrum does not originate from collision-induced dissociative ionisation of intact neutrals **1b**. It rather signifies dissociation of **1b** into α-pyridyl radicals which are subsequently collisionally ionised to yield *m/z* 78 ions. In this context, we note that the minimum energy requirement for the dissociation **1b** → [α-pyridyl]$^{\bullet}$ + OH$^{\bullet}$, is fairly low, ∼34 kcal/mol (from ΔH_f **1b** = 61 kcal/mol, this work and using ΔH_f **2a** = −18 kcal/mol [21], ΔH_f OH$^{\bullet}$ = 9 kcal/mol [21] and ΔH_f [α-pyridyl]$^{\bullet}$ = 86 kcal/mol [12b]).

The scenario that ions $\mathbf{1b}^{\bullet+}$ upon neutralisation partly remain intact but then completely isomerise into **1a** and partly decompose into α-pyridyl radicals, is fully supported by the computational results presented in Section 3.1: the barrier for the 1,3-H shift associated with the isomerisation **1b** → **1a** is fairly low,

~15 kcal/mol, whereas vertical neutralisation of **1b**$^{\bullet+}$ is expected to yield excited neutrals with minimum energies in the 10–20 kcal/mol range.

Structure characteristic intensity differences are also present in the CID spectra of **2a**$^{\bullet+}$ and its distonic isomers **2c**$^{\bullet+}$ and **2d**$^{\bullet+}$. Whereas the 2-hydroxypyridine ions **2a**$^{\bullet+}$ lose no H_2O, this reaction occurs in both distonic ions, as witnessed by the narrow peak at *m/z* 77. The distonic ions also lose COH$^{\bullet}$ much more readily to yield *m/z* 66 ions. They further share the weak but clearly discernable peak at *m/z* 44, which may well be a signature peak for the common structure element [HO–C=N–H]. Differences between the individual distonic ions are also evident, particularly in the *m/z* 41: *m/z* 28 peak intensity ratios. Assuming that these ions have the stable structures CH_2=C=N–H$^{\bullet+}$ and H–C=N–H^{+}, respectively, the large differences in these ratios correlate well with the proposed structures.

Ions **2c**$^{\bullet+}$ yield a NR spectrum with an intense survivor signal (see Fig. 2). Its NR/CID spectrum, see Fig. 1(b), is apart from the enhanced *m/z* 67 peak which results from the low-energy decarbonylation, virtually identical with the conventional CID spectrum. This attests to the isomeric purity of the source generated ions and moreover, it leaves little doubt that the neutral ylide is a stable species in the gas-phase.

Analysis of the NR and NR/CID spectra of isomer **2d**$^{\bullet+}$ is less straightforward. The ion–molecule reactions described in the next section remove any doubt that we are dealing with ions of structure **2d**$^{\bullet+}$ but, surprisingly, their NR spectrum displays a recovery signal of only marginal intensity. Analysis of the NR spectrum gives no indication that this can be attributed to a facile decomposition of the incipient neutrals by a simple bond cleavage, as proposed for isomer **1b**. However, as pointed out in the previous computational section, the incipient neutrals **2d** are expected to be generated with at least 0.5 eV (11.5 kcal/mol) of excess energy whereas the barrier for the 1,3-H shift leading to the very stable 2-pyridone isomer **2b** is only 13 kcal/mol. It is therefore, anticipated that the vertical neutralisation of **2d** largely yields 2-pyridone molecules which, see Table 1, contain at least 66 kcal/mol of excess energy. Such a high internal energy could suffice for their decarbonylation into 1-H pyrrole for which the minimum thermochemical energy requirement is ~18 kcal/mol [21]. This proposal implies that (i) the decarbonylation of *neutrals* **2b** and *ions* **2a**/**b**$^{\bullet+}$ is associated with the *same* large kinetic energy release, and (ii) that the NR spectrum contain a peak for CO$^{\bullet+}$ at *m/z* 28, which is as broad as the *m/z* 67 peak for ionised 1-H pyrrole. It is difficult to decide whether these conditions are met. The decarbonylation of 2-pyridone may well have a reverse activation energy, but the actual height of this barrier is not known. Further, the peaks in the *m/z* 25–29 region of the NR spectrum are not sufficiently resolved to establish whether the *m/z* 28 peak contains a broad component for CO$^{\bullet+}$.

An alternative explanation which we think is more likely, is that the incipient neutrals **2d** isomerise into pyridone molecules **2b**, which, because of their high internal energy content, readily decarbonylate as *ions* when ionised in the collisional ionisation step of the NR experiment. This tentative proposal is not incompatible with the 'noisy' NR/CID spectrum of the weak survivor ions: this spectrum, see Fig. 1(b), still shows tell-tale peaks at *m/z* 77 and 44 for the presence of ions **2d**$^{\bullet+}$ but their relative intensity has become lower and this is particularly true for the *m/z* 66 peak, compare the CID and NR/CID spectra of Fig. 1(b). From a comparison of the shapes of the *m/z* 67 peaks in narrow scans, it follows that those in the NR/CID spectra of ions **2d**$^{\bullet+}$ and **2a**$^{\bullet+}$ are closely similar. This supports the proposal that the weak survivor ions in the spectrum of **2d**$^{\bullet+}$ represent a mixture of ions **2d**$^{\bullet+}$ and **2b**$^{\bullet+}$. However, it also suggests that the large energy release associated with the decarbonylation is an inherent property of ions **2b**$^{\bullet+}$ rather than **2a**$^{\bullet+}$, as suggested in the previous section. More decisive evidence in favour of this proposal would come from a careful examination of the *metastable* ion spectrum of the **2d**$^{\bullet+}$ survivor ions, but unfortunately the signals in the NR/MI spectrum are too weak to permit a meaningful analysis.

Analysis of the spectra of the remaining distonic isomer, **3c**$^{\bullet+}$, is straightforward. Unlike its isomer **3a**$^{\bullet+}$, which shows a competitive loss of CO and HCN

in its MI spectrum, metastable ions **3c**$^{\bullet+}$ only undergo decarbonylation, most likely via the route **3c**$^{\bullet+}$ → (1,3-H) → **3b**$^{\bullet+}$ → [1-H pyrrole]$^{\bullet+}$ + CO. The kinetic energy release associated with this reaction is substantial, $T_{0.5} = 720$ meV, but nevertheless smaller than that for the decarbonylation of **3a**$^{\bullet+}$, $T_{0.5} = 780$ meV. This further underlines that isomerisation of the distonic ion into its more stable counterpart **3a**$^{\bullet+}$ via a 1,2-H shift does not occur to a significant extent. This is also borne out by the CID spectra of **3a**$^{\bullet+}$ and **3c**$^{\bullet+}$ (see Fig. 1(a)). Ions **3a**$^{\bullet+}$ have signature peaks at *m/z* 68 (loss of HCN) and *m/z* 55 (possibly hydroxy cyclopropenium ions, which also feature in the spectrum of **4a**$^{\bullet+}$) while the distonic ion features a much more pronounced *m/z* 28 peak, indicative of the presence of the [–CH–NH–] structure element in the ion. The NR spectrum of **3c**$^{\bullet+}$, see Fig. 2, displays an abundant recovery signal whose CID spectrum, see Fig. 1(a), is close to that of the source generated ions. Thus, these distonic ions retain their structure integrity in the NR experiment which signifies that their neutral counterpart is a stable species in the rarefied gas-phase.

3.4. Ion–molecule reactions with dimethyl disulfide

A complementary approach to the characterisation of isomeric ions involves probing differences in their reactivity by interactions with selected neutral molecules. One such molecule is dimethyl disulfide (DMDS), $CH_3S–SCH_3$ [26]. It was successfully used in recent work [27] to differentiate the pyridine radical cation from its α-ylide isomer. The pyridine ion readily undergoes charge exchange with DMDS, because pyridine's IE (9.3 eV) is higher than that of DMDS (8.0 eV [26]). The IE of pyridine's ylide isomer (6.8 eV) is lower than that of DMDS and thus, the ylide ions do not undergo charge exchange. Instead, they abstract a $CH_3S^{\bullet}$ radical from the DMDS to yield adduct ions whose structure was characterised by a subsequent high energy CID experiment.

In light of these interesting observations on the pyridine system, it seemed worthwhile to use DMDS in the present study as well. From the IE values reported in Table 2, it follows that the neutral counterparts of the ions of conventional structure, viz. **1a**$^{\bullet+}$, **2a**$^{\bullet+}$, **3a**$^{\bullet+}$ and **4a**$^{\bullet+}$ all have IEs higher than DMDS whereas the reverse obtains for the distonic ions **1b**$^{\bullet+}$, **2c**$^{\bullet+}$, **2d**$^{\bullet+}$ and **3c**$^{\bullet+}$.

Table 3
Product ions resulting from the interaction of various $C_5H_5NO^{\bullet+}$ ions with DMDS and *tert*-butyl isocyanide molecules

Substrate → ion	$CH_3S–SCH_3$		$(CH_3)_3C–NC$	
	m/z	*I* [a][a]	*m/z*	*I*[a]
1a$^{\bullet+}$	94 [DMDS]$^{\bullet+}$	200	57	0.3
			79	4
2a$^{\bullet+}$	94 [DMDS]$^{\bullet+}$	200	57	7
			84	10
3a$^{\bullet+}$	94 [DMDS]$^{\bullet+}$	160	57	1
			84	20
			121	2
4a$^{\bullet+}$	94 [DMDS]$^{\bullet+}$	300	57	1
			84	40
			121	40
1b$^{\bullet+}$	142 [**1b** + $CH_3S^{\bullet}$]$^{+}$	20	57	0.3
			84	0.2
			105	20
			121	5
2c$^{\bullet+}$	142 [**2c** + $CH_3S^{\bullet}$]$^{+}$	100	57	10
			84	30
			121	70
2d$^{\bullet+}$	142 [**2d** + $CH_3S^{\bullet}$]$^{+}$	40	57	2
			84	2
			121	10
3c$^{\bullet+}$	142 [**3c** + $CH_3S^{\bullet}$]$^{+}$	60	57	10
			84	20
			121	40

[a]Intensities relative to the main beam of reactant ions which was normalised to 1000 units.

The results of the ion–molecule reactions with DMDS are summarised in the left column of Table 3. It is seen that **1a**$^{\bullet+}$–**4a**$^{\bullet+}$ all undergo charge exchange, whereas the distonic ions all yield adduct ions at *m/z* 142 resulting from $CH_3S^{\bullet}$ abstraction. That the *m/z* 94 ions in the spectra of **1a**$^{\bullet+}$–**4a**$^{\bullet+}$ are DMDS$^{\bullet+}$ ions resulting from charge exchange and not $C_5H_4NO^{+}$ ions resulting from a $H^{\bullet}$ abstraction, readily follows from the sulphur characteristic *m/z* 94–96 peak intensity ratios observed.

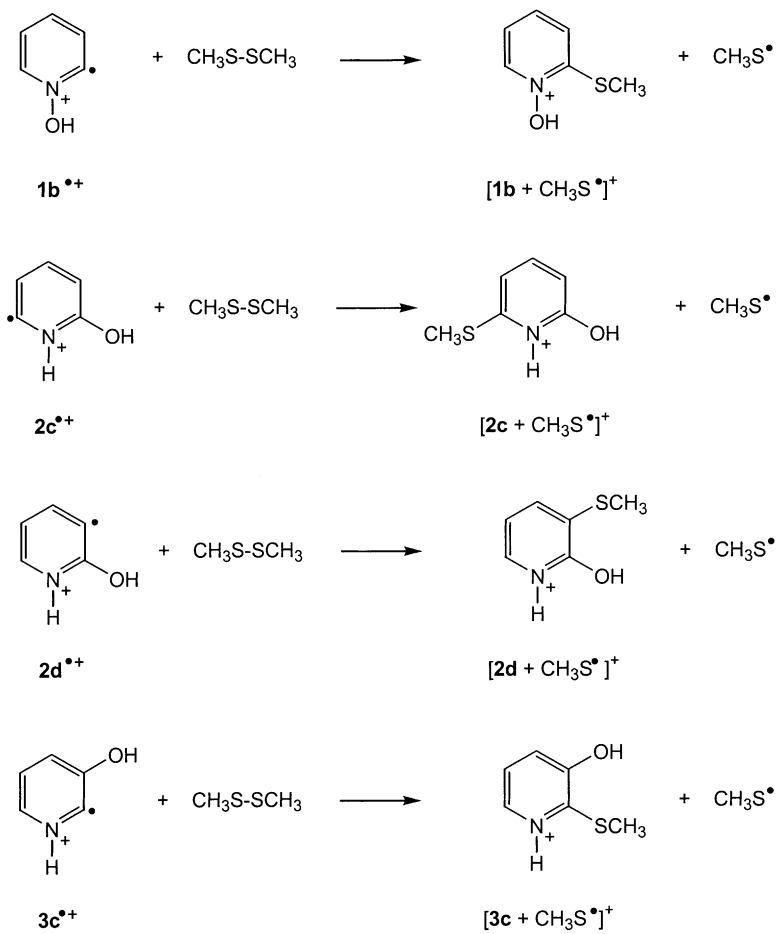

Scheme 5.

Structure proposals for the *m/z* 142 adduct ions generated from the distonic ions are presented in Scheme 5.

That all four reactions are exothermic is supported by our B3LYP/CBSB7 calculations which yield heat of reaction values of 35, 39, 37 and 38 kcal/mol, respectively. The high energy CID spectra of the four isomeric *m/z* 142 adduct ions are presented in Fig. 4.

These CID spectra are uniquely different. The adduct ions derived from $\mathbf{1b}^{\bullet+}$ show a prominent loss of H_2O (*m/z* 124) and also of $OH^{\bullet}$ (*m/z* 125). The latter ion uniquely characterises the $\mathbf{1b}^{\bullet+}$ isomer as does the *m/z* 79 peak which may originate from the consecutive loss of CH_2=S. The losses of $CH_3^{\bullet}$, H_2S and $CH_3S^{\bullet}$ yielding *m/z* 127, 108 and 95 ions, respectively, represent common dissociation pathways for the adduct ions from $\mathbf{2b}^{\bullet+}$, $\mathbf{2c}^{\bullet+}$ and $\mathbf{3c}^{\bullet+}$. However, the relative abundance is strongly isomer dependent as are the *m/z* 124 (loss of H_2O) and *m/z* 83 (loss of CS) peaks. The adduct ions $\mathbf{2}[\mathbf{c} + CH_3S^{\bullet}]^+$ lose both H_2O and CS whereas $[\mathbf{2d} + CH_3S^{\bullet}]^+$ loses no CS and loss of H_2O does not occur from $[\mathbf{3c} + CH_3S^{\bullet}]^+$. These observations can perhaps be correlated with the position of the OH– or CH_3S– substituent but, more importantly, they fully support the conclusion derived from the dissociation characteristics in the previous section that all four distonic ions are viable species in the gas-phase.

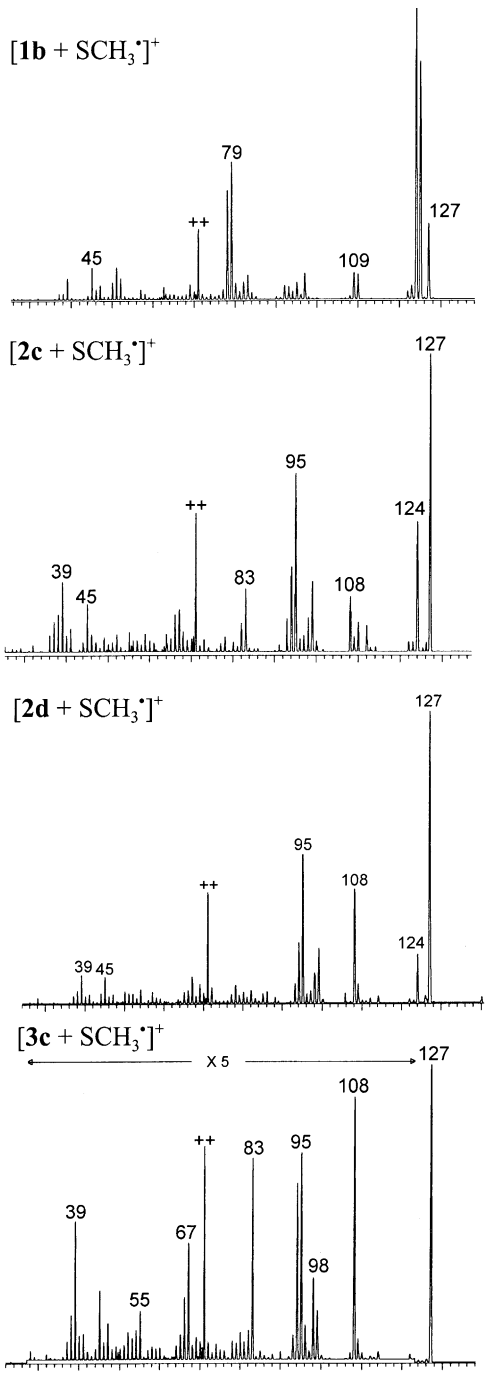

Fig. 4. Ion–molecule reactions between $C_5H_5NO^{\bullet+}$ radical cations (*m/z* 95) and dimethyl disulfide: the collision-induced dissociation spectra of the *m/z* 142 adduct ions generated from ions **1b**$^{\bullet+}$, **2c**$^{\bullet+}$, **2d**$^{\bullet+}$ and **3c**$^{\bullet+}$.

Another potentially useful substrate for isomer differentiation by ion–molecule reactions is *tert*-butyl isocyanide [28]. Its use in this study is described in Section 3.4.1.

3.4.1. Ion–molecule reactions of the $C_5H_5NO^{\bullet+}$ ions with tert-butyl isocyanide

Kenttämaa and co-workers [28] have recently investigated the reactivity of *tert*-butyl isocyanide towards various distonic radical cations. Two distinct reactivity patterns were observed, one characteristic of the electrophilic nature of the charge site of the ion, and the other characteristic of the unpaired spin of the free radical moiety. Reaction of the isocyanide with the charge site of the distonic ion involves CN^- transfer, yielding *m/z* 57 *tert*-$C_4H_9^+$ ions, while reaction at its radical site involves cyano radical transfer, yielding CN^- adduct ions. The isocyanide prefers to react at the distonic ion's charge site, but if this site is coordinately saturated, "chemically inert", reaction at the radical site becomes prevalent.

When the $C_5H_5NO^{\bullet+}$ isomeric ions of this study were allowed to interact with the isocyanide, several reactions were observed. From the results presented in Table 3, it follows that proton-transfer from the ion to the isocyanide, yielding $(CH_3)_3C–N{=}CH^+$ ions at *m/z* 84, and CN^- transfer, yielding *tert*-$C_4H_9^+$ ions at *m/z* 57, are common reactions for all isomeric ions but ion **1a**$^{\bullet+}$. The pyridine N-oxide ion is not deprotonated by the isocyanide, indicating that the associated C–H bond cleavage is less favoured than the O–H or N–H abstraction reactions occurring from the other isomers. Instead, ions **1a**$^{\bullet+}$ show another reaction which uniquely characterises them, viz. a deoxygenation reaction yielding pyridine ions and *tert*-butyl isocyanate neutrals. That the *m/z* 79 ions generated have the pyridine structure was confirmed by the analysis of the CID spectrum. We further note that the IE of pyridine (9.3 eV) is lower than that of the isocyanate (10.1 eV [21]) and thus, the charge remains on the reactant ion in the deoxygenation process. A second unique reaction, see Table 3, is the formation of *m/z* 105 ions from the ylide ion **1b**$^{\bullet+}$. The CID spectrum of these ions was obtained and it appeared to be virtually identical

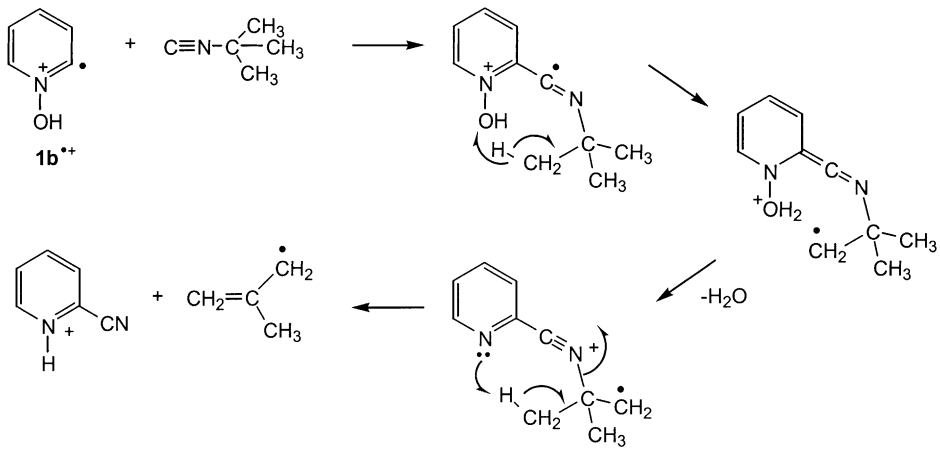

Scheme 6.

with that of the *m/z* 105 ions generated by the (ring N) protonation of 2-cyanopyridine. Having established the product ion structure, we tentatively propose that the ion is generated via the mechanism of Scheme 6. The first step involves formation of an adduct ion of **1b**$^{\bullet+}$ and the isocyanide. Consecutive H-transfers then lead to the losses of H_2O and $C_4H_7^{\bullet}$ to yield the N-protonated 2-cyanopyridine product ion at *m/z* 105.

Another prominent reaction of ions **1b**$^{\bullet+}$ with the isocyanide involves a $CN^{\bullet}$ transfer to the radical position of the ion, yielding **1**[**b** + $CN^{\bullet}$]$^{+}$ ions at *m/z* 121 and *tert*-butyl radicals. However, this is also a prominent reaction with the distonic ions **2c**$^{\bullet+}$, **2d**$^{\bullet+}$ and **3c**$^{\bullet+}$ and the 4-hydroxypyridine radical cation **4a**$^{\bullet+}$. The reaction is also observed with the 3-hydroxy isomer **3a**$^{\bullet+}$ but it is absent for **2a**$^{\bullet+}$. The proposed *m/z* 121 product ion structures are given in Scheme 7 and their CID spectra are presented in Fig. 5.

In the absence of detailed labelling experiments and thermochemical information about the various reaction products, a detailed analysis of these spectra remains speculative. Nevertheless, it is clear that the spectra are characteristically different. The CID spectrum of the adduct ion with **1b**$^{\bullet+}$ features an abundant loss of $OH^{\bullet}$ to yield 2-cyanopyridine ions at *m/z* 104. Loss of H_2O (*m/z* 103) is also observed but this reaction is only prominent for the distonic ions **2c**$^{\bullet+}$ and **2d**$^{\bullet+}$. These two isomers, however, can easily be differentiated on the basis of the *m/z* 66 and *m/z* 93 ions that dominate in the spectrum of **2d**$^{\bullet+}$. The *m/z* 66 ions are possibly HO–C≡C–C≡N$^{\bullet+}$, considering that they are also readily formed from [**3c** + $CN^{\bullet}$]$^{+}$, whereas those at *m/z* 93 could result from the loss of CO initiated by a 1,5-H transfer to the CN moiety of the ion.

Further, ions [**3a** + $CN^{\bullet}$]$^{+}$ and [**4a** + $CN^{\bullet}$]$^{+}$ which both contain an [NC–N=] moiety, appear to uniquely

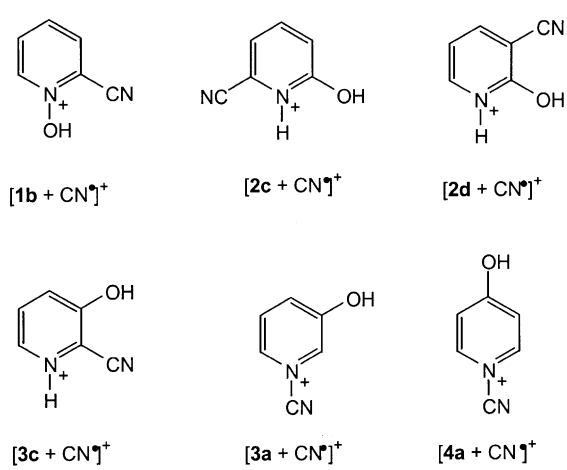

Scheme 7.

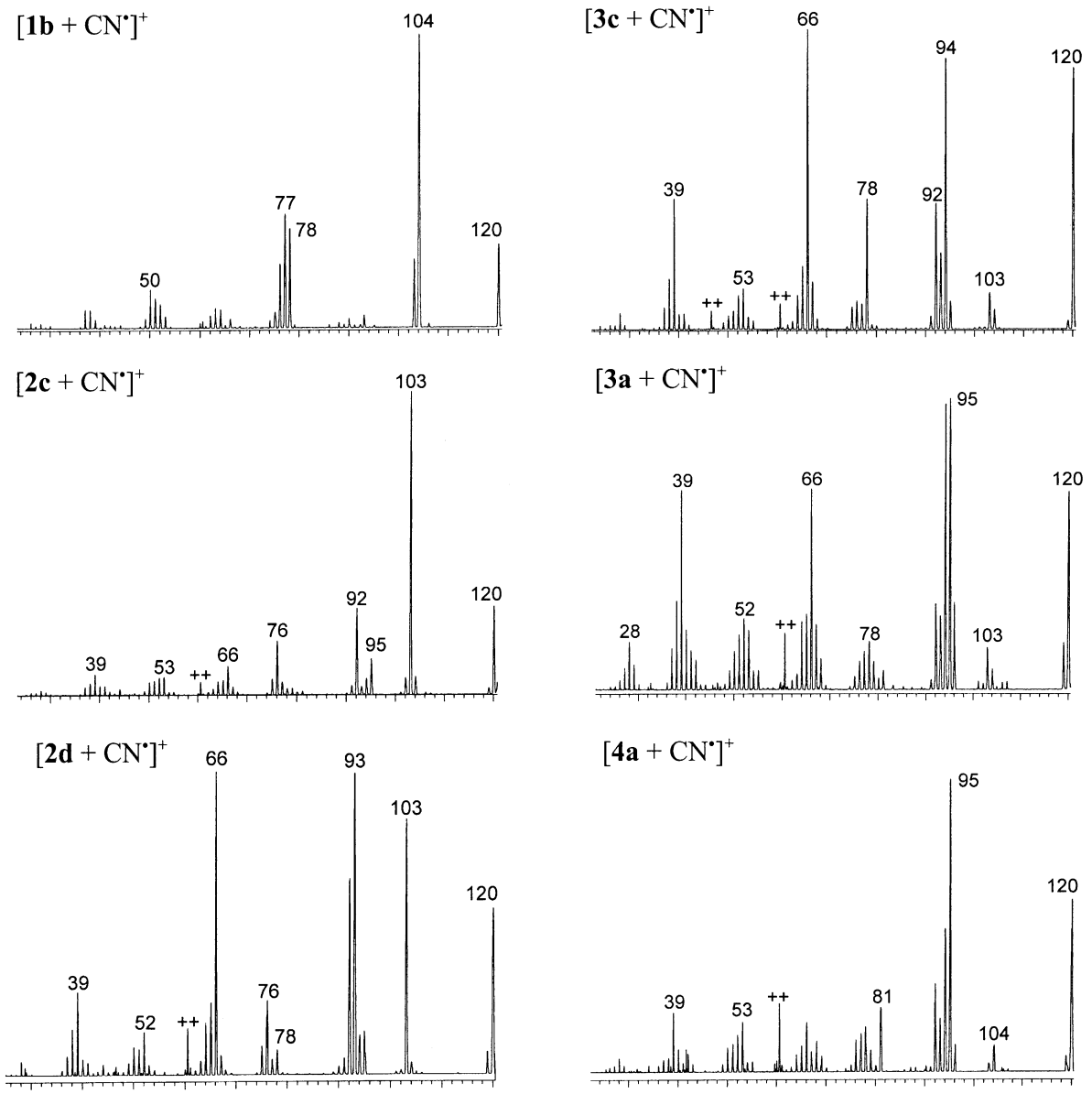

Fig. 5. Ion–molecule reactions between $C_5H_5NO^{\bullet+}$ radical cations (*m/z* 95) and *tert*-butyl isocyanide: the collision-induced dissociation spectra of the *m/z* 121 adduct ions generated from ions **1b**$^{\bullet+}$, **2c**$^{\bullet+}$, **2d**$^{\bullet+}$, **3c**$^{\bullet+}$, **3a**$^{\bullet+}$ and **4a**$^{\bullet+}$.

lose this structure element as NCN to yield *m/z* 81 ions, possibly having the structure of the hydroxy cyclopentenium ion [29].

Finally, we note that, although these associative ion–molecule reactions elegantly confirm the structure identity of the distonic ions, they do not allow us to decide whether the 2-hydroxy-pyridine ions are isomerically pure or actually consist of a mixture of keto and enol ions **2a**$^{\bullet+}$/**2b**$^{\bullet+}$ as discussed in Section 3.3.1.

4. Conclusions

The combined information from the dissociation and reactivity characteristics of the $C_5H_5NO^{\bullet+}$ ions studied, confirms our theoretical predictions that the distonic ions **1b**$^{\bullet+}$, **2c**$^{\bullet+}$, **2d**$^{\bullet+}$ and **3c**$^{\bullet+}$, depicted in Scheme 1, are stable species in the gas-phase. From the analysis of the recovery signals in their neutralisation–reionisation spectra, it follows that the neutral counterparts of **2c**$^{\bullet+}$ and **3c**$^{\bullet+}$ are also stable. In contrast, the ylide-type neutrals **1b** readily isomerise into pyridine N-oxide, **1a**, or else dissociate. The neutral counterparts of the distonic ions **2d**$^{\bullet+}$ have only a marginal stability and part of these neutrals are proposed to isomerise into energy-rich 2-pyridone molecules **2b**. This too, is in agreement with the computational results. Finally, we note that the question whether 2-hydroxypyridine yields isomerically pure ions **2a**$^{\bullet+}$ or, alternatively, a mixture of enol and keto (2-pyridone) ions, remains unresolved. Unlike the situation with the keto–enol isomeric pairs **3a**$^{\bullet+}$/**3b**$^{\bullet+}$ and **4a**$^{\bullet+}$/**4b**$^{\bullet+}$ whose CID spectra are characteristically different, enol ions **2a**$^{\bullet+}$ and keto ions **2b**$^{\bullet+}$ exhibit virtually the same dissociation characteristics.

Acknowledgements

The work at McMaster University was supported by the Natural Sciences and Engineering Research Council of Canada (NSERC). M.A.T. would like to thank NSERC for a Post Graduate Scholarship and McMaster University for a James A. Morrison Memorial Scholarship award. P.G. and R.F. thank the “Fonds National pour la Recherche Scientifique” for financial support in the acquisition of the tandem mass spectrometer.

References

[1] M. Gallant, T.P. Viet, J.D. Wuest, J. Am. Chem. Soc. 113 (1991) 721.
[2] P. Beak, Acc. Chem. Res. 10 (1977) 186.
[3] (a) U. Ohms, H. Guth, E. Hellner, H. Dannöhl, A.Z. Schwig, Z. Kristallogr. 169 (1984) 185;
(b) G.L. Wheeler, H.L. Ammon, Acta Crystallogr. Sect. B B30 (1974) 680.
[4] J. Wang, R.J. Boyd, J. Phys. Chem. 100 (1996) 1641.
[5] (a) P. Beak, F.S. Fry, J. Lee, F.J. Steele, J. Am. Chem. Soc. 98 (1976) 171;
(b) R.S. Brown, A. Tse, J.C. Vederas, J. Am. Chem. Soc. 102 (1980) 1174;
(c) S.S.T. King, W.L. Dilling, N.B. Tefertiller, Tetrahedron 28 (1972) 5859;
(d) C. Guimon, G. Garrabe, G. Pfister-Buillouzo, Tetrahedron Lett. 28 (1979) 2585.
[6] M.J. Cook, S. El-Abbady, A.R. Katritzky, C. Guimon, G. Pfister-Guillouzo, J. Chem. Soc. Perkin Trans II (1977) 1652.
[7] (a) J.R. Reimers, L.E. Hall, N.S. Hush, J. Phys. Chem. A 104 (2000) 5087;
(b) A.L. Sobolewski, L. Adamowicz, Chem. Phys. 213 (1996) 193;
(c) J.S. Kwiatkowski, J. Leszczynski, J. Mol. Struct. 376 (1996) 325;
(d) A.L. Sobolewski, L. Adamowicz, J. Phys. Chem. 100 (1996) 3933;
(e) R.J. Hall, N.A. Burton, I.H. Hillier, P.E. Young, Chem. Phys. Lett. 220 (1994) 129;
(f) O.G. Parchment, N.A. Burton, I.H. Hillier, Chem. Phys. Lett. 203 (1993) 46;
(g) M. Moreno, W.H. Miller, Chem. Phys. Lett. 171 (1990) 475;
(h) M.J. Scanlan, I.H. Hillier, Chem. Phys. Lett. 107 (1984) 330;
(i) M.J. Scanlan, I.H. Hillier, A.A. Macdowell, J. Am. Chem. Soc. 105 (1983) 3568;
(j) J.K. Wolken, F. Tureček, J. Phys. Chem. A 103 (1999) 6268;
(k) J.K. Wolken, F. Tureček, J. Am. Chem. Soc. 121 (1999) 6010.
[8] S. Suradi, N. El-Saiad, G. Pilcher, H.A. Skinner, J. Chem. Thermodyn. 14 (1982) 45.
[9] (a) A. Maquestiau, R. Flammang, Mass Spectrom. Rev. 1 (1982) 237;
(b) P.B. Terent’ev, A.G. Kalandarishuili, Mass Spectrom. Rev. 15 (1996) 339.
[10] (a) M.J. Cook, A.R. Katritzky, M. Taagepera, J. Am. Chem. Soc. 98 (1976) 6048;
(b) A. Maquestiau, Y. Van Haverbeke, C. De Meyer, A.R. Katritzky, M.J. Cook, A.D. Page, Can. J. Chem. 53 (1975) 490;
(c) A. Maquestiau, Y. Van Haverbeke, R. Flammang, H. Mispreuve, A.R. Katritzky, J. Ellison, J. Frank, Z. Meszarox, Chem. Commun. (1979) 888;
(d) T. Gronneberg, K. Undheim, Tetrahedron Lett. (1972) 3193;
(e) M.W.E.M. van Tilborg, J. van Thuijl, Org. Mass Spectrom. 18 (1983) 331.
[11] M.A. Baldwin, G.J. Langley, J. Chem. Soc. Perkin Trans. II (1988) 347.
[12] (a) D. Lavorato, J.K. Terlouw, T.K. Dargel, W. Koch, G.A. McGibbon, H. Schwarz, J. Am. Chem. Soc 118 (1996) 11898;

(b) M.A. Trikoupis, D.J. Lavorato, J.K. Terlouw, P.J.A. Ruttink, P.C. Burgers, Eur. Mass Spectrom. 5 (1999) 431;
(c) D.J. Lavorato, J.K. Terlouw, G.A. McGibbon, T.K. Dargel, W. Koch, H. Schwarz, Int. J. Mass Spectrom. Ion Proc. 179/180 (1998) 7;
(d) T.K. Dargel, W. Koch, D.J. Lavorato, J.K. Terlouw, H. Schwarz, Int. J. Mass Spectrom. 185–187 (1999) 925;
(e) D.J. Lavorato, T.K. Dargel, W. Koch, G.A. McGibbon, H. Schwarz, J.K. Terlouw, Int. J. Mass Spectrom., Nico Nibbering Honour Issue, in press.

[13] N. Goldberg, H. Schwarz, Acc. Chem. Res. 27 (1994) 34.

[14] (a) H.I. Kenttämaa, Org. Mass Spectrom. 29 (9) (1994) 1;
(b) L.A.B. Moraes, F.C. Gozzo, M.N. Eberlin, J. Org. Chem. 62 (1997) 5096;
(c) P. Gerbaux, Y. Van Haverbeke, R. Flammang, J. Mass Spectrom. 32 (1997) 1170.

[15] H.F. van Garderen, P.J.A. Ruttink, P.C. Burgers, G.A. McGibbon, J.K. Terlouw, Int. J. Mass Spectrom. Ion Processes 121 (1992) 159.

[16] (a) R.H. Bateman, J. Brown, M. Lefevere, R. Flammang, Y. van Haverbeke, Int. J. Mass Spectrom. Ion Processes 115 (1992) 205;
(b) R. Flammang, Y. van Haverbeke, C. Braybrook, J. Brown, Rapid Commun. Mass Spectrom. 9 (1995) 795.

[17] (a) J.A. Montgomery Jr., M.J. Frisch, J.W. Ochterski, G.A. Petersson, J. Chem. Phys. 112 (2000) 6532;
(b) J.A. Montgomery Jr., M.J. Frisch, J.W. Ochterski, G.A. Petersson, J. Chem. Phys. 110 (1999) 2822.

[18] Gaussian 98, Revision A.7, M.J. Frisch, G.W. Trucks, H.B. Schlegel, G.E. Scuseria, M.A. Robb, J.R. Cheeseman, V.G. Zarzewski, J.A. Montgomery Jr., R.E. Stratmann, J.C. Burant, S. Dapprich, J.M. Millam, A.D. Daniels, K.N. Kudin, M.C. Strain, O. Farkas, J. Tomasi, V. Barone, M. Cossi, R. Cammi, B. Mennucci, C. Pomelli, C. Adamo, S. Cliffrd, J. Ochterski, G.A. Petersson, P.Y. Ayala, Q. Cui, K. Morokuma, D.K. Malick, A.D. Rabuck, K. Raghavachari, J.B. Foresman, J. Cioslowski, J.V. Ortiz, A.G. Baboul, B.B. Stefanov, G. Liu, A. Liashenko, P. Piskorz, I. Komaromi, R. Gomperts, R.L. Martin, D.J. Fox, T. Keith, M.A. Al-Laham, C.Y. Peng, A. Nanayakkara, C. Gonzalez, M. Challacombe, P.M.W. Gill, B. Johnson, W. Chen, M.W. Wong, J.L. Andres, C. Gonzalez, M. Head-Gordon, E.S. Replogle, J.A. Pople, Gaussian Inc., Pittsburgh, PA, 1998.

[19] (a) S.J. Vosko, L. Wilk, M. Nusair, Can. J. Chem. 58 (1980) 1200;
(b) A.D. Becke, Phys. Rev. A 38 (1988) 5648;
(c) C. Lee, W. Yang, R.G. Parr, Phys. Rev. B 37 (1988) 785;
(d) A.D. Becke, J. Chem. Phys. 98 (9) (1993) 1372;
(e) A.D. Becke, J. Chem. Phys 98 (1993) 5648.

[20] H. Ozeki, M.C.R. Cockett, K. Okuyama, M. Takahashi, K. Kimura, J. Phys. Chem. 99 (1995) 8008.

[21] S.G. Lias, J.E. Bartmess, J.F. Liebman, J.L. Holmes, R.O. Levin, W.G. Mallard, J. Phys. Chem. Ref. Data 17 (Suppl. 1) (1988).

[22] R. Flammang, V. Henrotte, P. Gerbaux, M.T. Nguyen, Eur. Mass Spectrom. 6 (2000) 3.

[23] (a) J.L. Holmes, J.K. Terlouw, Org. Mass Spectrom. 15 (1980) 383;
(b) J. Laskin, C. Lifshitz, J. Mass Spectrom. 36 (2001) 459.

[24] R. Buff, J. Dannacher, Int. J. Mass Spectrom. 62 (1984) 1.

[25] J.L. Holmes, J.K. Terlouw, J. Am. Chem. Soc. 101 (1979) 4973.

[26] D.T. Leeck, H.I. Kenttämaa, Org. Mass Spectrom. 29 (1994) 106.

[27] P. Gerbaux, M. Barbieux-Flammang, J.K. Terlouw, R. Flammang, Int. J. Mass Spectrom. 206 (2001) 91.

[28] E.D. Nelson, R. Li, H.I. Kenttämaa, Int. J. Mass Spectrom. 185–187 (1999) 91.

[29] S.J. Blanksby, S. Dua, J.H. Bowie, D. Schröder, H. Schwarz, J. Chem. Phys. A 104 (2000) 11248.